Mechanism of enhancement in absorbance of vibrational bands of adsorbates at a metal mesh with subwavelength hole arrays

Junji Etou,[a] Daisuke Ino,[b] Daisuke Furukawa,[a] Kazuya Watanabe,[ac] Ikuyo F. Nakai,[a] and Yoshiyasu Matsumoto*[a]

Received Xth XXXXXXXXXX 20XX, Accepted Xth XXXXXXXXX 20XX
First published on the web Xth XXXXXXXXXX 200X
DOI: 10.1039/b000000x

We have investigated the mechanism of enhanced absorption intensities of vibrational bands of adsorbates on copper meshes with subwavelength holes by measuring and simulating temporal profiles of infrared pulses transmitted through the meshes. As reported previously [Williams *et al., J. Phys. Chem. B*, 2003, **107**, 11871], the absorption intensities of CH stretching bands of alkanethiolate adsorbed on the mesh increase substantially with decreasing hole size. The enhancements of absorption intensities are associated with temporal delays of infrared pulses transmitted through the mesh. Finite difference time domain calculations reproduce the observed pulse delays as a function of hole size. These facts indicate that the delays of transmitted pulses are not caused by coupling of infrared radiation to surface plasmon polaritons propagating on the front and rear surfaces of the mesh, but they are caused by the reduction in group velocity owing to coupling to waveguide modes of mesh holes. Consequently, the strong enhancements of the absorption intensities are attributed to adsorbates inside the holes rather than to those on the mesh surfaces that have been proposed previously.

1 Introduction

It is attractive to apply surface electromagnetic waves (SEWs) to vibrational spectroscopy of adsorbate, because SEWs propagating along surfaces provide long interaction path lengths and hence high detection sensitivity. Because SEW dispersion curves lie below the light line, various coupling schemes have been developed for propagation of SEWs on metal surfaces with the aid of prisms and gratings, etc.[1–3]

Using metal meshes with subwavelength periodic hole arrays, Coe and co-workers have recently developed another scheme to launch SEWs on metal surfaces for vibrational spectroscopy of adsorbates in the mid infrared (IR) range.[4–6] They revealed that adsorption on metal meshes greatly enhances the intensities of absorption bands of adsorbates.[4] The absorbance of alkanethiolate self-assembled monolayer is of order 10^{-1} in the wide frequency range: $700 - 3000\ \mathrm{cm}^{-1}$; this is by more than two orders of magnitude larger than the absorbance usually observed with IR absorption reflection spectroscopy (IRAS) for adsorbates on flat metal surfaces.[7]

The enhanced absorption of adsorbates was closely related to extraordinary transmission (EOT) of light through a perforated metal film with a periodic subwavelength hole array, which was first reported by Ebbesen and co-workers.[8–10] Various theoretical models have been developed, and it is now generally accepted that SEWs including surface plasmon polariton (SPP) play an important role in EOT.[11,12] A periodic pattern of a metal mesh allows IR radiation to couple to SPPs effectively if the momentum of SPP matches the momenta of the incident light and the mesh.[13] At the normal incidence to the metal mesh with a two-dimensional square array as depicted in Fig. 1, the momentum conservation at the mesh dictates that SPPs are excited resonantly at around

$$\lambda_{ij} = \frac{L n_{\mathrm{eff}}}{\sqrt{i^2 + j^2}}, \qquad (1)$$

where L is the period of the square array, n_{eff} is the real part of an effective index of refraction of the interface between metal and dielectrics, and i and j are scattering orders of the array.[8] For example, a strong resonance peak appears at λ = 12.7 μm in zero-order transmission spectra of a Ni mesh with L = 12.7 μm and a hole width a = 6.5 μm.[4,5] This resonance peak is assignable to (i, j) = (1,0). Resonance peaks become broader and overlap each other with increasing scattering orders. Thus, the transmission spectra have no distinct resonance peaks as the IR wavelength becomes shorter.

Coe and co-workers adapted the SPP coupling scheme proposed by Ebbesen and co-workers: SPPs excited by incident IR radiation propagate on the incident plane of the mesh, couple to SPPs at the rear surface via waveguide modes inside holes, and then emit photons. Because propagating SPPs can

[a] *Kyoto University, Kyoto 606-8502, Japan. Fax: +81 (0)75 753 4050; Tel: +81 (0)75 753 4047; E-mail: matsumoto@kuchem.kyoto-u.ac.jp*
[b] *Panasonic Corporation, 3-4 Hikaridai, Seika-cho, Soraku-gun, Kyoto 619-0237, Japan.*
[c] *PRESTO-JST, 4-1-8 Honcho Kawaguchi, Saitama, 332-0012, Japan.*

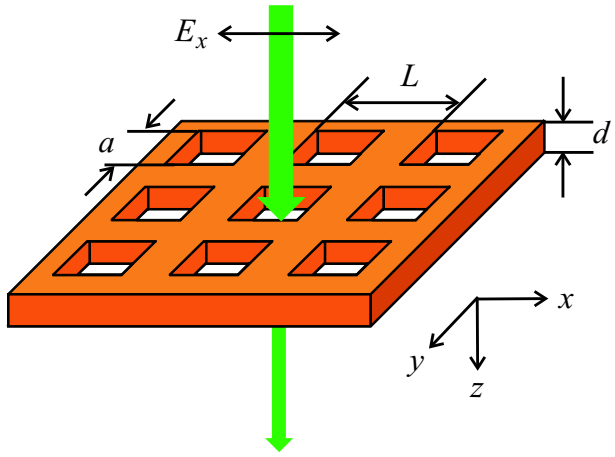

Fig. 1 Schematic representation of a copper mesh with periodic square holes. L is the period of the square array, a is the hole width, and d is the thickness of the mesh. The IR beam polarised along x is directed perpendicularly to the mesh surface.

interact with adsorbates on the surfaces of meshes, the interaction length becomes substantially longer. Thus, the enhanced absorbance of adsorbate vibrational bands was attributed to effectively elongated interaction lengths with the aid of coupling of IR radiation to SPP modes.[5,14]

This plausible mechanism of enhanced IR absorption, however, does not necessarily explain consistently all the experimental results obtained so far. First, a critical test for the proposed mechanism is to examine how enhanced absorption intensities depend on the propagation lengths of SPPs. Williams et al.[15] reported that the absorption intensities of vibrational bands of formaldehyde on metal meshes are greatly enhanced in the wide IR frequency range from 900 to 3500 cm^{-1}. Because the wavelengths and intensities of SPP resonances change with the incident angle of IR radiation, the absorption intensities would also vary significantly with incident angle; but this did not happen.[15] Second, because the absorption band of the CH_2 rocking mode of hexadecane is close to the (1,0) resonance of a Ni mesh with $L = 12.7$ μm, it is appropriate to examine how the absorption band intensity changes when the resonance wavelength is tuned across the centre of the absorption band. Again, this test failed to show that the exact resonance condition gives a maximum absorption intensity.[5,16] Third, using IR imaging spectroscopy, Coe and co-workers have recently estimated the propagation lengths of SPPs on the similar metal meshes;[17] the measurements indicated that the relative absorption intensities do not correlate the propagation lengths. As a result, they argued that the lateral propagation of SPPs along the mesh surfaces are not responsible for most of the IR absorption enhancements reported by them.[17] Therefore, the mechanism of enhanced IR absorption of adsorbates on metal meshes has not been fixed yet.

To examine the validity of the proposed mechanism, we need to investigate how coupling of IR radiation to SEWs at metal meshes enhances the absorption intensities of adsorbate vibrational bands. We took a time domain approach to tackle this problem. Only a few studies have been conducted for measurements of temporal profiles of light pulses transmitted through subwavelength hole arrays. At $\lambda \sim 800$ nm, transit times of 7–10 fs were reported for perforated silver[18] and gold films.[19] The delay times were directly related to the lifetimes of resonant SPP modes, corresponding to a propagation length of a few μm. In the mid-IR range, however, no time-domain measurements have been performed for metal films with subwavelength hole arrays to the best of our knowledge. This paper reports measurements and finite difference time domain (FDTD) calculations of temporal profiles of IR pulses transmitted through metal meshes that exhibit enhanced adsorbate absorption. We show that adsorbates inside holes largely contribute to enhancements in IR absorption at $\lambda \sim 3$ μm rather than those on the front and rear surfaces of meshes.

2 Methods

It is essential to measure how absorption intensities and temporal profiles of IR beams transmitted depend on the hole width of a mesh. We controlled the hole width in a similar manner used by Williams et al.[20] Copper was deposited electrochemically onto a copper mesh with square holes (Precision Eforming, $L = 12.7$ μm, $a = 7$ μm, $d = 4$ μm). A piece of the mesh was located at ~ 4 mm away from a circular copper electrode with a diameter of 5 mm. A constant voltage of 10 V was applied to the copper electrode in an aqueous solution composed of 0.44 mol/dm^3 $CuSO_4$, 2.0 mol/dm^3 H_2SO_4 and 1.4 mmol/dm^3 HCl. The hole width decreased with increasing deposition time: it took ~ 2 min for $a = 3$ μm and 4 min for $a = 1$ μm. With this method we prepared meshes with a hole width in the range of 1 – 6.5 μm. The hole width was measured with a scanning electron microscope. A standard deviation of hole width was 0.2 μm for each mesh. Surface roughness of meshes after the electrochemical treatment was monitored by an atomic force microscope (AFM).

Monolayers of alkanethiolate on mesh surfaces were prepared in the following. The mesh was dipped in an ethanol solution of dodecanethiol (1 mmol/dm^3) for more than three hours. The solution was placed inside an ultrasonic bath. This ultrasonic stimulation helped to some extent to reduce variations in adsorbate absorbance for meshes having a similar hole width. The mesh was thoroughly rinsed by ethanol after removed from the solution for elimination of dodecanethiol multilayers.

Absorption spectra of dodecanethiolate adsorbed on mesh surfaces were measured with a Fourier-transformed infrared

(FTIR) spectrometer (Nicolet 6700). The mesh sample was placed in an N_2-purged sample chamber of the FTIR spectrometer. The IR beam was directed along the surface normal of the mesh and the transmitted beam was monitored with a mercury-cadmium-telluride detector.

The temporal profile of IR pulses transmitted through the mesh was measured as follows. A part of the output of a Ti:sapphire regenerative amplifier (Spectra Physics, λ = 800 nm, 1 kHz repetition rate, $\sim$ 150 fs duration) generated a broad band IR pulse (280 fs duration, centred at $\sim$3000 cm^{-1}) with a home-made optical parametric amplifier system and a difference frequency generator with $AgGaS_2$. The transmitted IR pulse through the mesh and a rest of 800-nm pulse were overlapped to each other onto a $LiNbO_3$ crystal for sum frequency generation. The up-converted signal intensity was measured with a photomultiplier (Hamamatsu C7169) as a function of delay between the two pulses. The measurements of cross correlation between 800-nm and IR pulses provided the pulse shape and delay of transmitted IR pulses.

FDTD calculations were performed for simulating the temporal profile of transmitted IR pulses and spatial distributions of electric field components at the mesh by using the package of FullWave (RSoft Inc.). The grid size for FDTD calculations depending on the hole width was chosen: 0.2 μm for $a \geq 3$ μm and $a/15$ for $a < 0.1$ μm. The Drude model was used for the frequency dependence of the permittivity of copper,

$$\varepsilon(\omega) = 1 - \frac{\omega_p^2}{\omega(\omega + i\gamma)}, \qquad (2)$$

where ω_p is the plasma frequency and γ is the phenomenological bulk electron relaxation rate. The data of the permittivity of copper were taken from the literature.[21] Fitting them to Eq. (2) in the wavelength range from 0.4 to 10 μm resulted in $\omega_p = 1.068 \times 10^{16}$ and $\gamma = 1.386 \times 10^{14}$ rad/s.

3 Infrared absorption spectra of alkanethiolate

Reducing the hole width to less than 3 μm, we observed absorption spectra showing large absorption intensities and spectral features that are almost identical to those reported by Coe and co-workers.[4] Fig. 2(a) shows an absorption spectrum taken from the mesh of a = 1.4 μm covered with dodecanethiolate. The absorption bands at 2849 and 2917 cm^{-1} are due to CH symmetric (d^+) and asymmetric stretching (d^-) of methylene in the alkyl chain, respectively, and the weak band at $\sim$ 2960 cm^{-1} is due to asymmetric stretching of methyl (r^-). The spectral features are very different from those obtained for monolayers on flat metal surfaces;[7] the spectra observed in the current study show that the absorption bands of CH_3 are much weaker than those of CH_2. In particular, the Fermi resonance pair of CH_3 symmetric stretch at $\sim$ 2880 and $\sim$ 2935 cm^{-1} is almost completely missing. These features are very similar to those observed for crystallines of long, all-trans n-alkanes pressed in a KBr pellet.[22] This suggests that alkanethiolate adsorbates in the current and previous studies[4] do not form a well-ordered monolayer at mesh surfaces.

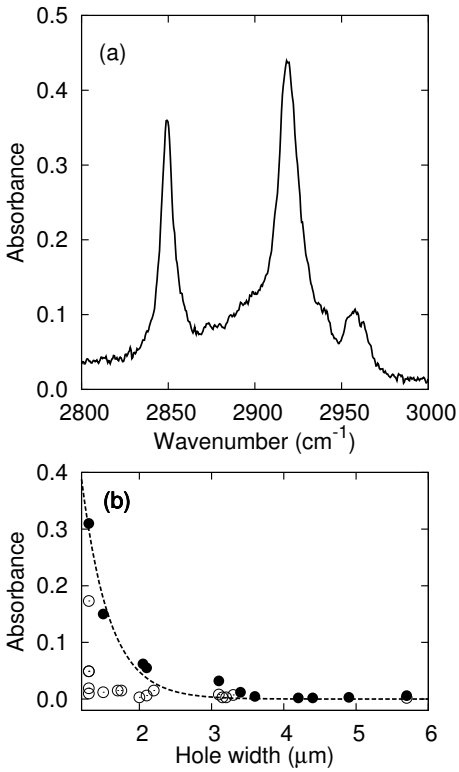

Fig. 2 (a) Absorption spectrum of dodecanethiolate adsorbed on a Cu mesh with a hole width of 1.4 μm. (b) Absorbance of the CH_2 asymmetric stretching band as a function of hole width. Data showing the largest absorbance among meshes with a similar hole width are marked by solid circles. The dashed line is a result of fitting the data marked by solid circles with eq. (6).

As shown in Fig. 2(b), some meshes with hole widths less than 2 μm showed anomalously large absorbance of d^- band: it exceeds 0.1. Because mesh surfaces after the electrochemical treatment become rough, we first examine the effect of surface-enhanced infrared absorption (SEIRA).[23–26] The surface roughness was estimated from AFM images. Flat copper surfaces after the same electrochemical treatment for meshes showed corrugations of $\pm$50 nm in average. A typical lateral dimension of protrusions was 300 nm. We estimated the SEIRA effect due to the surface roughness by making a comparison between two surfaces: flat copper surfaces with and without electrochemical deposition of a copper thin film. Both surfaces were covered with a monolayer of dodecanethiolate and IRA spectra were taken at grazing incidence of IR light. The absorbance of d^- band at the surface with electrochemical

deposition is 1.4×10^{-2}; this is larger than that of the surface without electrochemical deposition by a factor of 20. This enhancement factor due to SEIRA is typically observed at rough surfaces. Thus, the SEIRA effect could be partly responsible for the absorbances observed in meshes. However, the significantly larger absorbances observed for the meshes with $a < 3$ μm cannot be explained solely by the SEIRA effect.

The measurements of absorption intensities were problematic. As noted by Coe and co-workers,[5] we also found that absorption intensities varied widely from sample to sample as shown in Fig. 2(b). Meshes with a similar hole width showed very different absorption intensities, although they were treated through the same dipping procedure in the alkanethiol solution. Variations in absorbance were particularly large for the meshes with tiny holes with a hole width less than ~ 2 μm. As we describe later, the anomalously large enhancements in absorbance are mainly caused by molecules adsorbed inside holes. Thus, the absorption intensities depend on a couple of factors relating to the structure of mesh holes. First, the roughness inside mesh hole surfaces governs the number of alkanethiolate molecules adsorbed. Second, as the hole size becomes smaller, holes more likely trap air inside; this makes the solution difficult to wet the interior of holes. Ultrasonic stimulation of meshes in the alkanethiol solution was not effective enough to reproduce absorption intensities. Some subtle differences in surface roughness inside mesh holes would affect wetting of holes and the amount of adsorbates on the inside walls of holes.

Under the circumstances, averaging the absorbance data taken from all the samples with a certain hole width is meaningless, because the sample conditions, particularly the number of adsorbed molecules in mesh holes, are seemingly very different from sample to sample. Although absorption intensities scatter widely, it is worth noting that large enhancements in absorbance were only observed for meshes of $a \leq 2$ μm. Moreover, as marked by solid circles in Fig. 2(b), the data set showing the largest absorbance among meshes with a similar hole width gives a clear tendency: absorbance increases steeply as the hole width becomes smaller. Thus, we focused on the data set marked by solid circles hereafter.

4 Temporal profiles of transmitted pulses

Coupling to SEWs including SPP modes at a mesh with subwavelength holes strongly affects the temporal profile of IR pulses transmitted. Thus, temporal profile measurements of transmitted IR pulses provide a useful clue to study the coupling of IR radiation to SEWs. Fig. 3(a) shows an observed temporal profile of pulses transmitted through the mesh of $a = 1.4$ μm in comparison with that of pulses travelling in air without the mesh in the optical path. The pulses transmitted through the mesh were clearly delayed by 60 fs.

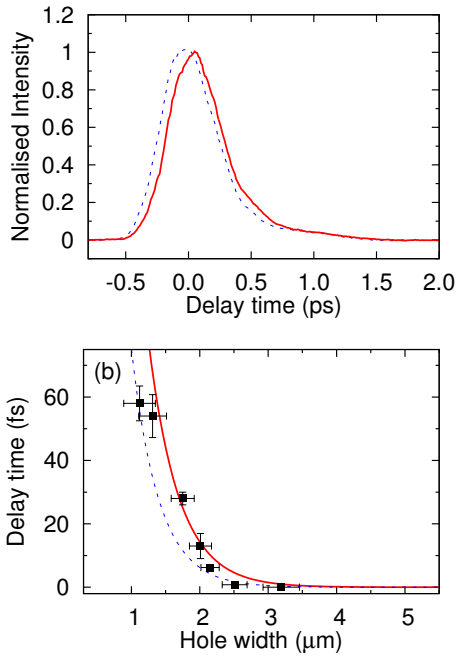

Fig. 3 (a) Temporal profiles of IR pulses of λ= 3.4 μm transmitted through the copper mesh (red solid line) and one travelling in air without passing through the mesh (blue dashed line). The mesh has a period of a square array of 12.7 μm and a hole width of 1.4 μm. Intensity is normalised at the peak of each profile. (b) Delay times observed (solid square) plotted against the hole width. Delay times calculated with FDTD are depicted for the mesh of 5 μm thick (blue dashed line) and 10 μm thick (red solid line).

Temporal profile measurements were performed as a function of hole width from $a = 1.1$ to 3.2 μm. Delay times observed are plotted in Fig. 3(b). They increase nonlinearly as the hole width decreases. This indicates that the transmission through the mesh reduces the propagation speed of IR pulses. To estimate quantitatively a degree of speed reduction, we need to know the thickness of meshes. In general, meshes become thicker as the hole width decreases by electrochemical deposition. Roughly speaking, the thickness of mesh increases as much as decrease in the hole width:

$$d = d_0 + (a_0 - a), \tag{3}$$

where d_0 = 4 μm and a_0 = 7 μm are the thickness and the hole width of the mesh before any electrochemical deposition, respectively. Thus, the thickness of the mesh of a = 1.4 μm is estimated to be d = 9.6 μm. Because a transit time of light through the air gap of 9.6 μm is 32 fs, the total elapsed time required for the light pulse to transmit through the hole of the mesh is 92 fs. This corresponds to a group velocity of $\sim 0.4c$, where c is the velocity of light in vacuum; this is substantially slower than those measured for gold and silver meshes upon incidence of optical pulses at $\lambda \sim$800 nm.[18,19]

5 FDTD simulations

FDTD simulations help our understanding of temporal profiles and delays of transmitted IR pulses observed. The geometry of Cu mesh used in the FDTD simulations is depicted in Fig. 1. While the period of square arrays was fixed at L =12.7 μm, the hole width was changed systematically. Incident IR pulses, propagating along z with linear polarisation along x, have a Gaussian profile with a duration of 280 fs. For comparison, simulations were performed at the centre wavelength of $\lambda = 3.4$ μm in addition to $\lambda = 12.7$ μm at which a strong (1,0) SPP resonance is expected.

At $\lambda = 12.7$ μm, FDTD simulations show a strong coupling of IR radiation to SPPs that propagate on both front and rear mesh surfaces with significantly long lifetimes. An instantaneous spatial distribution of the electric field E_z of SPP excited by the incident IR pulse is depicted in Figs. 4(a) and (b). This snap shot was taken at the moment close to the peak of the incident pulse. The E_z amplitude is mainly distributed at the hole edges, and it remains large (not shown) even after the interaction with the incident pulse is over. As described later (cf. Fig. 5(b)), the prolonged oscillating E_z at the hole edges forms a dipole field that emits IR photons: an origin of EOT. At λ = 3.4 μm, by contrast, SPPs are hardly launched at the mesh surfaces. As shown in Figs. 4(c) and (d), a distribution pattern of E_z appears at the hole edges similar to the case of λ = 12.7 μm, but this field component only exists while the mesh is irradiated with the incident pulse. Note that the E_z field strength scatters into air, indicating that the E_z field at the mesh surfaces is effectively damped radiatively. Figs. 4(e) and (f) show an instantaneous spatial distribution of E_x at λ = 3.4 μm. While the light pulse transmits through the hole, the oscillating E_x field is built on the inner surfaces of the hole due to coupling with waveguide modes.

The interactions between the incident pulse and the mesh affect the temporal profile of transmitted pulses. Fig. 5(a) shows the temporal profile of the IR pulse at λ = 12.7 μm transmitted through a single hole of a = 7 μm and d = 5 μm. This is very identical to the incident pulse. In contrast, when the periodic boundary condition is applied, i.e., in the case of mesh with a two-dimensional periodic hole array, the IR pulse transmitted through the mesh has a retarded component as shown in Fig. 5(b). As described in the previous paragraph, this retarded component is attributable to SPPs launched on the mesh surfaces. The SPP waves at the incident plane resonantly excited by the IR pulse pass through holes via waveguide modes inside the hole and store a part of the energy to the SPP waves at the rear surface. These SPP waves emit IR radiation, while they couple to each other. This kind of temporal profiles of transmitted pulses has been observed in the THz range.[27] Thus, the retarded component is a good indicator for the coupling of IR pulses to SPP modes.

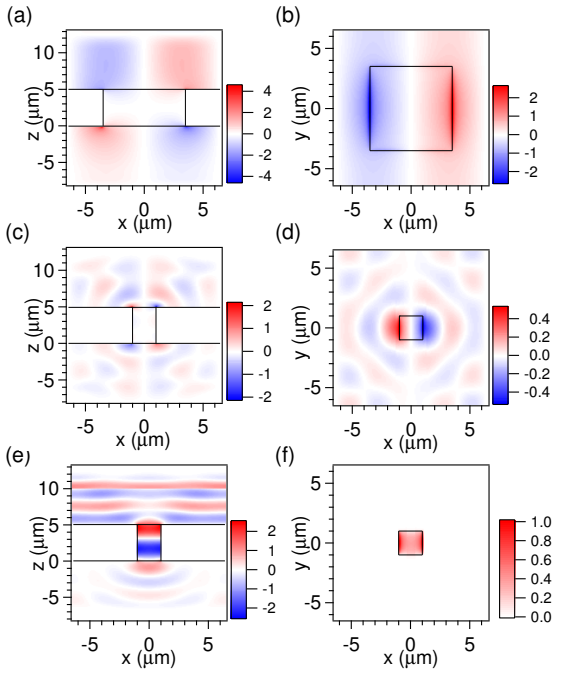

Fig. 4 Instantaneous spatial distributions of electric fields at mesh surfaces. The mesh has dimensions of L = 12.7 and d = 5 μm. The IR pulse linearly polarised along x is directed perpendicularly to the mesh from $z > 0$ to $z < 0$. (a) and (b) E_z component for λ = 12.7 and a = 7 μm; (c) and (d) E_z component for λ = 3.4 and a = 2 μm; and (e) and (f) E_x component for λ = 3.4 and a = 2 μm. (a), (c), and (e) are cross sectional views at the hole centre, y = 0 μm; (b), (d), and (f) are lateral views at the incident surface of the mesh, z = 5 μm. The distributions are taken at the moment close to the peak of the incident pulse.

In contrast to the case of λ = 12.7 μm, the temporal profile of the transmitted pulse at λ = 3.4 μm is not altered significantly. Fig. 5(c) shows the temporal profile of an IR pulse transmitted through the mesh with a = 2 μm and d = 5 μm: the transmitted pulse does not show any noticeable retarded components. This indicates that the incident IR radiation at λ = 3.4 μm does not couple effectively to SEWs at the mesh surfaces. Instead, the transmitted pulse was delayed from the one propagating freely in air without passing through the mesh as a result of coupling to waveguide modes inside holes.

Delay times obtained from FDTD calculations are depicted in Fig. 3(b) as a function of hole width. Considering the mesh thickness used in the measurements, we performed calculations for the meshes with d = 5 and 10 μm. Clearly delay times increase with decreasing hole width for both the meshes, and the 10-μm thick mesh has a longer delay time than the 5-μm thick mesh at each hole width. Note that the delay times observed fall in the range of delay times calculated for the meshes of d = 5 and 10 μm. This indicates that the observed

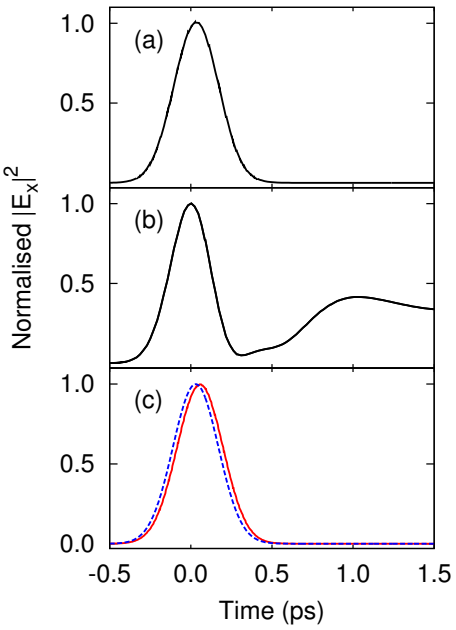

Fig. 5 Temporal profiles of IR pulses transmitted through Cu meshes calculated with FDTD simulations. The incident IR pulse is polarised along x (see Fig. 1) and has a pulse width of 280 fs. The square amplitude $|E_x|^2$, normalised at its maximum, is plotted as a function of time. The period of square arrays and the thickness of meshes are fixed at L = 12.7 μm and d = 5 μm, respectively. (a) λ = 12.7 μm, a single hole with a = 7 μm; (b) λ = 12.4 μm, a periodic hole array with a = 7 μm; (c) λ = 3.4 μm, a periodic hole array with a = 2 μm (red) and the pulse travelling in air without passing through the mesh (blue) .

delay times can be accounted for by the coupling of incident IR radiation to waveguide modes in mesh holes.

6 Mechanism of enhancement of absorbance

The FDTD simulations at $\lambda = 12.7$ μm show that the IR pulse couples substantially with SPP modes that propagate on both the front and rear surfaces of mesh. Since this makes effective optical path length longer, the mechanism proposed by Coe and co-workers would be reasonable around this wavelength. However, both the aforementioned experimental and simulation results at $\lambda = 3.4$ μm indicate that the coupling to SPP modes is very ineffective at this wavelength. Thus, the observed anomalously strong absorption of CH stretching bands cannot be accounted for by the same mechanism. Here we discuss another possible mechanism.

There are two possible origins of modulation of temporal profiles of IR pulses: couplings to SPPs at air/mesh interfaces and to waveguide modes inside the hole. Kim et al.[19] showed that 40-fs pulses at λ= 790 nm transmitted through a perforated Ag film were delayed by about 10 fs; the delays are attributed to the resonant couplings to SPP modes. According to the FDTD simulation results, however, IR pulses at λ= 3.4 μm cannot excite SPP modes effectively at the mesh currently used. Thus, the couplings of SPPs at air/mesh interfaces do not contribute to the observed delay times. Instead, the coupling to waveguide modes inside the holes of a mesh contribute to the retardation of pulses.

Cutoff wavelengths of a rectangular metallic hole with horizontal and vertical dimensions $a \times b$ are determined by the two integers m and n:[28,29]

$$\lambda_c = \left[\left(\frac{m}{2a} \right)^2 + \left(\frac{n}{2b} \right)^2 \right]^{-1/2}. \quad (4)$$

The group velocity v_g decreases as the wavelength of incident light λ approaches to the cutoff wavelength as

$$v_g = c \left[1 - \left(\frac{\lambda}{\lambda_c} \right)^2 \right]^{1/2}. \quad (5)$$

Thus, the elapsed time of incident IR pulses through the mesh holes becomes longer. This is the origin of delays observed in the measurements and the FDTD simulations. Interactions with copper and alkanethiolate adsorbates at hole walls introduce an energy loss of IR light. Gallot et al.[29] showed that the absorption coefficient during propagation of light through the waveguide with a thin dielectric layer is proportional to $1/v_g$. Because v_g becomes smaller when the wavelength of incident light approaches the cutoff wavelength of the waveguide, the loss by the thin layer significantly increases.

The coupling of IR pulses to waveguide modes can be interpreted as coupling to long-lived quasistationary states (or trapped modes) of an electromagnetic cavity, known as scattering resonances in quantum mechanical scattering theory. Borisov et al.[30] demonstrated that trapped modes due to resonances in nanostructured materials with a periodic pattern play a key role in EOT. Following this theory, we can regard each mesh hole as a cavity. The Q of the cavity can be written as[28] $Q = \omega/\Gamma$, where $\omega = 2\pi c/\lambda$ is the resonance frequency and $\Gamma = 2\pi/\tau$ is the width. Assuming that the IR pulses at λ = 3.4 μm couple to waveguide modes of the mesh hole and that τ is given by the delay time, 60 fs, we estimated the effective Q factor to be ~ 5 for the mesh hole with a = 1.4 μm.

The FDTD calculations depicted in Fig. 3(b) give the hole-width dependence of the delay time. Let $f(a)$ be the delay time per unit distance along the hole axis of a mesh with the hole width a. Then, the elapsed time of the pulse per unit distance becomes $1/v_g = f(a) + 1/c$. The second term $1/c$ stems from the elapsed time of the pulse propagating through the air gap of unit distance. This term contributes to absorbance in the limit where the hole width is so large that no signifi-

cant pulse retardations take place. We neglect this contribution to absorbance, because this is much smaller than that of the retarded light pulse coupled with waveguide modes of tiny holes, where absorbance is significantly enhanced. Thus, the hole-width dependence of absorbance $\alpha(a)$ for the IR pulse propagating through the hole can be written as:

$$\alpha(a) = Adcf(a), \tag{6}$$

where A is the absorption constant. Taking into account for the hole-width dependence of d in Eq. (3), we fitted a set of the absorbance data marked with solid circle in Fig. 2(b) to Eq. (6). A reasonably good fitting was obtained with $A = (1.44 \pm 0.08) \times 10^{-2}$ μm^{-1}, as depicted in Fig. 2(b). Thus, we conclude that the coupling with waveguide modes inside the mesh hole is responsible for the enhanced absorbance observed.

7 Conclusions

We have observed strong enhancements in absorption intensities of C-H stretching bands of alkanethiolate adsorbed on copper meshes with subwavelength hole arrays. This finding is in qualitative agreement with the works reported previously. The time profile of IR pulses at λ = 3.4 μm transmitted through the meshes does not show any retarded components due to coupling of IR radiation to SPPs at the front and rear surfaces of the mesh, but show substantial delay times as the hole width becomes small. This is because the group velocity decreases at the wavelength close to the cutoff wavelength of the hole. Therefore, the anomalous absorption of IR by adsorbates stems from coupling of incident IR light to waveguide modes rather than elongated optical path lengths due to coupling to SPP modes propagating on both the front and rear surfaces of the mesh.

Acknowledgements

This study is supported in part by Grants-in-Aid for Scientific Research (S) (Grant No. 17105001) and (A) (Grant No. 2224501) from the Japan Society for the Promotion of Science, and the industry-academia collaboration with Panasonic Inc. K. W. gratefully acknowledges financial support by the PRESTO program of JST.

References

1 A. Otto, *Z. Phys.*, 1968, **216**, 398.
2 E. Kretschmann and H. Raether, *Z. Naturforsch.*, 1968, **A 23**, 2135.
3 J. Schoenwald, E. Burstein and J. M. Elson, *Solid State Commun.*, 1973, **12**, 185.
4 S. Williams, A. Stafford, K. Rodriguez, T. Rogers and J. Coe, *J. Phys. Chem. B*, 2003, **107**, 11871.
5 J. Coe, K. Rodriguez, S. Teeters-Kennedy, K. Cilwa, J. Heer, H. Tian and S. Williams, *J. Phys. Chem. C*, 2007, **111**, 17459.
6 J. V. Coe, J. M. Heer, S. Teeters-Kennedy, H. Tian and K. R. Rodriguez, *Annu. Rev. Phys. Chem.*, 2008, **59**, 179.
7 P. E. Laibinis, G. M. Whitesides, D. L. Allara, Y. T. Tao, A. N. Parikh and R. G. Nuzzo, *J. Am. Chem. Soc.*, 1991, **113**, 7152.
8 H. F. Ghaemi, T. Thio, D. E. Grupp, T. W. Ebbesen and H. J. Lezec, *Phys. Rev. B*, 1998, **58**, 6779.
9 T. W. Ebbesen, H. J. Lezec, H. F. Ghaemi, T. Thio and P. A. Wolff, *Nature*, 1998, **391**, 667.
10 C. Genet and T. W. Ebbesen, *Nature*, 2007, **445**, 39.
11 F. J. G. de Abajo, *Rev. Mod. Phys.*, 2007, **79**, 1267.
12 F. J. Garcia-Vidal, L. Martin-Moreno, T. W. Ebbesen and L. Kuipers, *Rev. Mod. Phys.*, 2010, **82**, 729.
13 H. Raether, *Surface Plasmons on Smooth and Rough Surfaces and on Gratings*, Springer-Verlag, 1988.
14 S. M. Teeters-Kennedy, K. R. Rodriguez, T. M. Rogers, K. A. Zomchek, S. M. Williams, A. Sudnitsyn, L. Carter, V. Cherezov, M. Caffrey and J. V. Coe, *J. Phys. Chem. B*, 2006, **110**, 21719.
15 S. Williams, K. Rodriguez, S. Teeters-Kennedy, A. Stafford, S. Bishop, U. Lincoln and J. Coe, *J. Phys. Chem. B*, 2004, **108**, 11833.
16 K. R. Rodriguez, H. Tian, J. M. Heer, S. Teeters-Kennedy and J. V. Coe, *J. Chem. Phys.*, 2007, **126**, 151101.
17 K. E. Cilwa, K. R. Rodriguez, J. M. Heer, M. A. Malone, L. D. Corwin and J. V. Coe, *J. Chem. Phys.*, 2009, **131**, 061101.
18 A. Dogariu, T. Thio, L. J. Wang, T. W. Ebbesen and H. J. Lezec, *Opt. Lett.*, 2001, **26**, 450.
19 D. S. Kim, S. C. Hohng, V. Malyarchuk, Y. C. Yoon, Y. H. Ahn, K. J. Yee, J. W. Park, J. Kim, Q. H. Park and C. Lienau, *Phys. Rev. Lett.*, 2003, **91**, 143901.
20 S. M. Williams, K. R. Rodriguez, S. Teeters-Kennedy, S. Shah, T. M. Rogers, A. D. Stafford and J. V. Coe, *Nanotechnology*, 2004, **15**, S495.
21 *Handbook of Optical Constants of Solids*, ed. E. D. Palik, Academic, Orlando, 1985.
22 R. A. MacPhail, H. L. Strauss, R. G. Snyder and C. A. Elliger, *J. Phys. Chem.*, 1984, **88**, 334.
23 A. Hatta, T. Ohshima and W. Suëtaka, *Appl. Phys. A*, 1982, **29**, 71.
24 M. Osawa and M. Ikeda, *J. Phys. Chem.*, 1991, **95**, 9914.
25 M. Osawa, K.-I. Ataka, K. Yoshii and Y. Nishikawa, *Appl. Spectrosc.*, 1993, **47**, 1497.
26 M. Osawa, *Bull. Chem. Soc. Jpn.*, 1997, **70**, 2861.
27 T. H. Isaac, W. L. Barnes and E. Hendry, *Phys. Rev. B*, 2009, **80**, 115423.
28 J. D. Jackson, *Classical electrodynamics*, John Wiley & Sons, Inc., 3rd edn, 1999.
29 G. Gallot, S. P. Jamison, R. W. McGowan and D. Grischkowsky, *J. Opt. Soc. Am. B*, 2000, **17**, 851.
30 A. G. Borisov, F. J. García de Abajo and S. V. Shabanov, *Phys. Rev. B*, 2005, **71**, 075408.

A table of contents entry

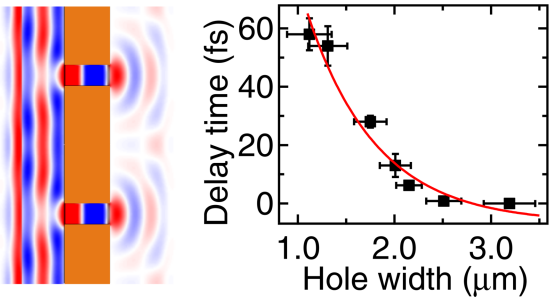

Infrared absorption of adsorbates on meshes with subwavelength hole arrays are enhanced by coupling of IR light to waveguide modes of mesh holes.